LIGHT-EMITTING DIODES

A light-emitting diode (LED) is nothing more than a semiconductor p–n junction that emits visible, infrared, or ultraviolet radiation. This is a result of injection of electrons and holes into a region of the semiconductor where they recombine and in the process emit photons with energy nearly equal to the bandgap. For light emitters, LEDs are no exception, direct bandgap semiconductors are chosen in which the recombination process is very efficient. The III–V semiconductors such as GaAs, GaP, AlGaAs, InGaP, GaAsP, GaAsInP, and AlInGaP are the common constituents used for LEDs. However, which material should be used for which type of LED depends on the desired color, performance, and cost.

Inside the prominent epoxy dome, a typical semiconductor chip embodying an LED has a size of $250 \times 250\ \mu m^2$ and is mounted on one of the electrical leads. The top of the chip is electrically connected to the other lead through a bond wire. The epoxy dome serves as a lens to focus the light and hold the package together, as depicted in Fig. 1. For red LEDs, which are the most common, the usual operating currents are approximately 10 mA to 50 mA and a forward voltage is approximately 2 V.

The external quantum efficiency is defined as the number of photons produced for each electron passing through the device. In the absence of external losses this figure also is a measure of the power efficiency of an LED, and ranges from less than 0.1% to more than 10%. In visible LEDs, however, the perception by a human eye is the determining parameter, not the power measured in a laboratory setting. Consequently, the luminous performance of visible LEDs is obtained by multiplying the power efficiency by the eye sensitivity curve; the efficacy curve, which is defined by the Commission Internationale de L'Eclairage, or CIE. Moreover, photometric terms such as lumens and lumens per watt, in place of radiometric

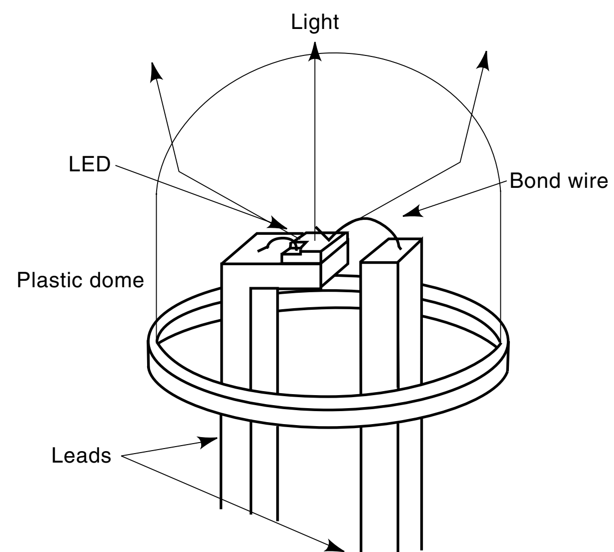

Figure 1. Schematic diagram depicting the epoxy package containing an LED.

J. Webster (ed.), *Wiley Encyclopedia of Electrical and Electronics Engineering*. Copyright © 1999 John Wiley & Sons, Inc.

terms such as watts and power efficiency, are used as figures of merit for power and efficiency of an LED. The performance of visible LEDs is typically in the range of 1 lm/W to 10 lm/W, although performances as high as 20 lm/W have been achieved in the spectral region with good eye sensitivity. This is comparable to the 10 lm/W to 15 lm/W performance of an incandescent bulb. Because they canoperate even at less than 0.1 W, LEDs are suitable for low level room illumination. The wider appeal of LEDs, however, is in the areas of large-area displays, traffic lights, moving signs, exterior lighting on vehicles, and potentially for lighting (1).

High-volume production of LEDs was implemented in 1968 following the introduction of GaP : (Zn,O) LEDs (2). Both GaAsP and GaP : (Zn,O) LEDs exhibited an efficiency of about 0.1 lm/W and were available only in red. In the late 1960s and early 1970s, it was discovered that nitrogen can provide an efficient recombination center in both GaP and GaAsP (3,4). This discovery led to the commercialization of red, orange, yellow, and green GaAsP : N and GaP : N LEDs with a performance improvement of approximately 1 lm/W. Later, it was discovered that both homostructure AlGaAs and heterostructure AlGaAs LEDs are capable of offering potential performance advantages over GaAsP and GaP homojunction LEDs (5). But, it was not easy to produce AlGaAs-based devices at high volume and low cost because liquid-phase-epitaxy (LPE) reactors, which were employed at the time, capable of growing high-quality multilayered device structures were cumbersome. As a result, these LEDs did not become commercially available until the early 1980s when the production problems were solved with the advent of metal organic vapor phase epitaxy (MOVPE). The performance of these red LEDs was significantly improved, ranging from 2 lm/W to 10 lm/W depending upon the structure employed. Thus, for the first time, LEDs broke the efficiency barrier of filtered incandescent bulbs, enabling them to replace light bulbs in many outdoor display applications.

As a result of relentless development efforts, AlInGaP based orange and yellow LEDs with efficiencies above 10 lm/W were developed in the early 1990s (6). Interestingly, conventional techniques such as LPE or halide-transport vapor phase epitaxy (HVPE) proved intractable for the growth of these LEDs. Again, the MOVPE method was eventually employed for a more controlled growth of heterostructure AlInGaP LEDs. The performance of these LEDs was satisfactory. Although the available green LEDs were adequate, the missing link to full color displays was a blue LED. In the early 1990s SiC-based LEDs emerged as potential blue color emitters to fill that gap (7). The SiC carbide LEDs had to rely on donor acceptor transitions in an indirect semiconductor with resulting low efficiencies and brightness.

This necessitated the use of five or more SiC LEDs for each red LED for color balance. The stage was therefore set for the development of brighter blue and green LEDs using III–V nitride and ZnSe based semiconductors (8). Successful laboratory demonstrations in 1990 eventually led to the emergence of nitride-based LEDs in the marketplace for bright blue and green LEDs in 1993 and 1994, respectively.

A DEVICE PHYSICS PRIMER

p–n Junctions

The structure of an LED comprises a single *p–n* junction as previously indicated and as appears in Fig. 2. When this junction is forward biased, electrons are injected into the *p*-type region and holes are injected into the *n*-type region. The injected minority carries recombine with majority carriers, releasing energy, which in direct bandgap semiconductors is primarily in the form of photons. Heterojunction varieties are more efficient as electrons and holes are confined, placing them close to one another. Moreover, the active layer can be lightly doped, and both types of carriers can be injected efficiently from the barrier layers. The turn-on voltage for substantial current flow ranges from 0.8 eV to 1.5 eV for infrared emission, from 1.5 eV to approximately 3.0 eV for visible emission, and larger than 3.5 eV for ultraviolet emission. The reverse breakdown voltage is generally determined by the carrier concentration in the region with heavier doping, which is generally the *n*-type region. It ranges from 5 V to 10 V for heavily doped devices, and to more than 50 V for visible LEDs utilizing large bandgap semiconductors in which carriers require larger energies for avalanche breakdown.

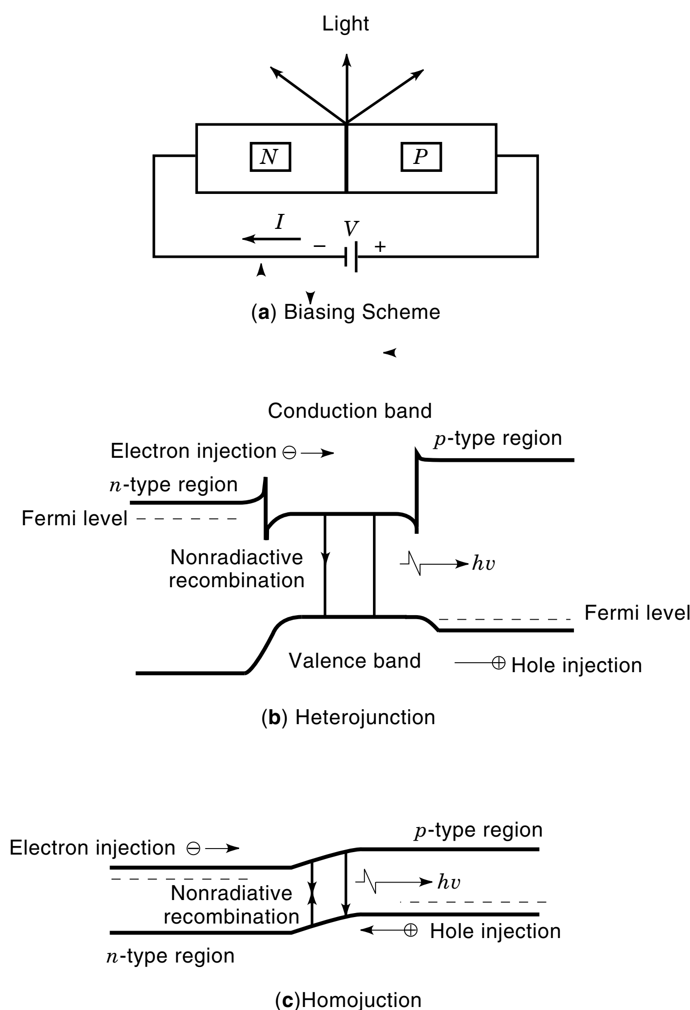

Figure 2. Schematic diagram of a *p–n* junction forward-biased LED, (a) biasing conditions, (b) heterojunction, (c) homojunction.

The slope of the current-voltage characteristics after they are turned on in the forward direction yields the dynamic resistance. This resistance is determined by the area of the junction, the ohmic-contact technology, and the conductivity of the semiconductor materials involved. The dynamic resis-

tance is about 1 Ω for a high-current-operation infrared LED. For a visible LED optimized to yield high light output at 30 mA or less, this dynamic resistance can be more than 10 Ω. It should be noted that the power drop across this resistance is a pure loss that degrades the wall-plug efficiency of the device.

Radiative and Nonradiative Recombination and Internal Quantum Efficiency

When injected minority carriers recombine with majority carriers, the energy can be converted into light or heat. Heat is released when the recombination is nonradiative, which is undesirable. The energy is given off as light if the recombination is radiative. The internal quantum efficiency of an LED is given by the number of photons generated over the number of injected minority carriers. In other words, it is determined by the radiative recombination over all the recombination events. Thus, the performance of an LED would be high if the nonradiative carrier lifetime τ_{nr} were much larger than the radiative carrier lifetime τ_r. The nonradiative lifetime τ_{nr} of carriers is a function of the quality of the material, and is generally in the tens of nanoseconds for good materials. If the nonradiative path is minimized, τ_{nr} can be as large as a microsecond or even larger. Unlike τ_{nr}, τ_r should be as small as possible for a high efficiency LED. If B is the recombination rate constant for a given semiconductor material, and n and p are the electron and hole concentrations in the recombination region, then at low minority carrier injection levels, the radiative recombination rate may be given by $n/\tau_r = Bnp$ so that $\tau_r = (Bp)^{-1}$. It is therefore, apparent that to minimize τ_r, the hole concentration p should be as large as possible without degrading the quality of the material and decreasing τ_{nr}. Unfortunately, the material quality degrades if it is doped beyond a certain maximum hole concentration ($\sim 10^{17}$ to 10^{19} cm^{-3}, depending on the material) which causes τ_{nr} to decrease rather sharply. Thus the doping level must be optimized.

The radiative constant B is material dependent and assumes the value of about 2×10^{-10} cm^3/s for GaAs. Thus, for $p = 10^{18}/cm^{-3}$, which is the usual hole density in the p region, the radiative decay time for a GaAs device is approximately $\tau_r = (Bp)^{-1} = 5 \times 10^{-9}$ s. The nonradiative decay time τ_{nr} for the same GaAs is $\sim 10^{-7}$ or longer. These values of τ_r and τ_{nr} yield an internal quantum efficiency approaching 100%. For most materials the situation is, however, far from ideal. Because of low material quality and the fact that the recombination rate is smaller, the internal quantum efficiency in these semiconductors is much lower than 100%. This is particularly true for indirect bandgap semiconductors for which B is several orders of magnitude smaller. The external quantum efficiency is defined as the internal quantum efficiency multiplied by the light extraction factor. The light extraction from the interior of an LED chip is difficult to determine, because the light emission is random in direction. Thus, the external quantum efficiency can also be lower than the internal quantum efficiency by more than an order of magnitude.

MODEL

To put forth a theoretical model (9) for various parameters of an LED, let us consider a p–n junction LED (see Fig. 2) that is forward biased and has n and p regions doped relatively heavily. As the active region is p-type, we will effectively deal with electrons as minority carriers. Assuming a one-dimensional transport equation, the continuity equation for these electrons can be expressed as:

$$D\left(\frac{\partial^2 n}{\partial x^2}\right) - \frac{n - n_0}{\tau} + g = \left(\frac{\partial n}{\partial t}\right) \tag{1}$$

where n and n_0 are the instantaneous and equilibrium minority carrier concentrations, respectively. Among others, D, g, and τ are the electron diffusion coefficient, generation rate, and the carrier lifetime, respectively, and x is the distance.

If we consider steady-state conditions and large injection levels, which generally prevail for LEDs, the time dependence of carrier concentration n, the generation rate g, and the equilibrium minority carrier concentration n_0 become negligible. All these lead Eq. (1) to reduce to

$$D\left(\frac{d^2 n}{dx^2}\right) - \frac{n}{\tau} = 0 \tag{2}$$

The general solution of Eq. (2) is

$$n(x) = A\exp\left(\frac{-x}{L}\right) + B\exp\left(\frac{x}{L}\right) \tag{3}$$

where A and B are the unknown constants to be determined by the boundary conditions, and L is the minority carrier diffusion length, $L = (D\tau)^{1/2}$. In the p region,

$$n(x) = A\sinh\left(\frac{w-x}{L}\right) + B\cosh\left(\frac{w-x}{L}\right) \tag{4}$$

For an LED, the rate of change of carrier concentration at $x = 0$ is the difference between the injection rate and interface recombination rate. The rate of change of carrier concentration at $x = w$ is the difference between injection rate at $x = w$ and interface recombination rate at $x = w$. More specifically,

$$-\left(\frac{dn}{dx}\right)_{x=0} = \frac{J_{\text{diff}}(0)}{qD} - \frac{v_s n(0)}{D}, \quad \text{at } x = 0 \tag{5}$$

and

$$-\left(\frac{dn}{dx}\right)_{x=W} = \frac{J_{\text{diff}}(w)}{qD} - \frac{v_s n(w)}{D}, \quad \text{at } x = w \tag{6}$$

where q is the electronic charge, J_{diff} is the diffusion current density, and v_s is the interface recombination velocity (cm/s). As is apparent from Eqs. (5) and (6), the rate of change of the minority carrier is always negative. Furthermore, if the p layer is thicker than the diffusion length, the diffusion current J_{diff}(w) is negligible.

With the help of Eqs. (5) and (6), the solution to the continuity equation is obtained as

$$n(x) = \frac{\xi_d J_{\text{diff}}(x=0)}{q}\left\{\frac{\cosh\left(\frac{w-x}{L}\right) + \xi_d v_s \sinh\left(\frac{w-x}{L}\right)}{(\xi_d v_s^2 + 1)\sinh\left(\frac{w}{L}\right) + 2\xi_d v_s \cosh\left(\frac{w}{L}\right)}\right\} \tag{7}$$

where $\xi_d = (\tau/D)^{1/2}$. Also, $J_{diff}(x = 0)$ is the value of J_{diff} at $x = 0$. As the hole injection is negligibly small, this $J_{diff}(x = 0)$ can be assumed to be identical to the terminal current.

The average electron concentration in the active region can then be calculated from

$$\overline{n} = \frac{1}{w}\int_0^w n(x)\,dx = \frac{J\tau_{\text{eff}}}{qw} \tag{8}$$

The substitution of the electron concentration from Eq. (7) into Eq. (8) leads the effective carrier lifetime to be

$$\tau_{\text{eff}}^{-1} = \tau^{-1} + 2\left(\frac{v_s}{w}\right) = \tau_{\text{rad}}^{-1} + \tau_{\text{nrad}}^{-1} + 2\left(\frac{v_s}{w}\right) \tag{9}$$

Note that, if $(w/L) < 1$, $(\xi_d^2 v_s^2) \ll 1$. Furthermore, in the absence of interface recombination, the effective lifetime reduces to τ.

DEVICE STRUCTURES

The LED business is a very cost driven one and as such the simplest and the least expensive LEDs win out. Homojunctions in which the entire epitaxial structure, and sometimes the substrate, consists of the same compound or alloy are therefore desirable unless heterojunctions can be produced with similar ease or cost. The p–n junction can be formed by p-type diffusion into an n-type epitaxial film or can be grown by changing the dopant type during the epitaxial growth process. In terms of the fabrication issues, there is not much cost difference between the homo- and heterojunction devices, and yet the heterojunctions can offer several additional advantages. For example, carrier injection can be more efficient in a heterostructure LED than in a homostructure LED. The LED structure with the best efficiency is, however, a double heterostructure, that is, one in which an active region possessing a lower energy gap is sandwiched between two cladding layers of higher energy gaps. Among them, the upper one is called the *window layer* and the lower one the *confining layer*. If the cost of production is acceptable, which fortunately is the case owing to recent developments in epitaxial deposition techniques, a double heterostructure LED has the advantage of reduced absorption of the generated radiation. The active region of this LED can be made quite thin, typically 0.01 μm to 3 μm. The thinner this layer, the smaller is the self-absorption. The carrier confinement coupled with low interface recombination velocity insures that the recombination takes place predominantly in the active region. The confinement of the carriers to a narrow region also results in fast and efficient recombination because of the proximity of the electrons and holes.

LEDs made of one or more quantum wells have also been fabricated. However, it is noted that advantages do not outweigh the associated complications. Consequently, devices of this type are not widely used in LED applications at the present time.

SEMICONDUCTOR MATERIALS USED

An ideal compound or alloy composition for an LED is one that exhibits an energy band gap E_g suitable for the desired emission wavelength. It should preferably have a direct energy gap and be doped easily, both n and p type. For infrared (IR) and red emission, E_g should be less than 2 eV, a range possessed by GaAs, AlGaAs, and GaAsP (with Al or P mole fraction $x \le 0.4$ (see Table 1). If the energy bandgap of the chosen compound is larger than desired, the emission energy must be reduced by introducing non-band-edge recombination centers such as isoelectronic dopants which also have the added benefit of increasing the radiative recombination efficiency. This is indeed a very useful technique because indirect bandgap materials such as GaP and GaAsP ($x > 0.5$) can be widely used for LEDs if doped with isoelectronic impurities such as nitrogen. LEDs emitting in orange, red, and yellow colors can be made also from AlInGaP alloy system ($E_g \sim 2.0$ eV). Although many II–VI materials such as ZnSe have a large enough direct bandgap, it has not been possible to form suitable p–n junctions until recent developments in ZnSe.

Ideally, the substrate for an LED should have low defect levels, be lattice matched to the epitaxial layers, and be transparent to the emitted radiation. Unfortunately, it is not always possible to satisfy all these conditions simultaneously, and a trade-off becomes inevitable. Consequently, when GaAs, GaP, and InP are grown with some degree of cost-effectiveness, the defect levels remain high, and yet low enough to yield good LEDs. If silicon is used as a substrate for GaAs devices, the GaAs layers turn out highly defective from poor lattice mismatch.

PERFORMANCE CHARACTERISTICS OF VISIBLE LIGHT EMITTING DIODES

The luminous performance of various LEDs is summarized in Table 2. Among the LEDs tabulated, the $Al_xGa_{1-x}As$, $(Al_xGa_{1-x})_yIn_{1-y}P$, and InGaN based commercial LEDs demonstrate the best performances and quantum efficiencies at their respective wavelengths. This is most likely because these aforementioned LEDs satisfy most of the desired design criteria, such as direct energy bandgap of the active region, employment of double heterostructures, and, in the case of the conventional III–V semiconductors, lattice matching with the substrates. At the present time, $Al_xGa_{1-x}As$ and $(Al_xGa_{1-x})_yIn_{1-y}P$ LEDs are relatively expensive as compared to GaP based ones and are used only for special-purpose applications such as high-density optical read-and-write technologies. Lower cost homojunction GaAsP and GaP LEDs, although inferior in quality, dominate the high-volume applications. Improved production practices are beginning to reduce the cost.

GaAsP- and GaAsP : N-Based Light Emitting Diodes

For a phosphorus mole fraction $x \le 0.45$, $GaAs_{1-x}P_x$ is a direct energy gap semiconductor, and hence $GaAs_{1-x}P_x$ LEDs can emit in the IR and red spectral regions. These are homojunction devices with diffused junctions patterned by photolithographic means. As a result, they are very suitable for applications that require small emitting areas and/or more than one emitting region on each LED chip. As GaAs and GaP have substantially different lattice parameters, the $GaAs_{1-x}P_x$ alloy system is not lattice matched to GaAs (or GaP) substrates. This leads to high defect density and internal absorption of light, which lowers the efficiency. Nevertheless, $GaAs_{1-x}P_x$

Table 1. Important Materials for LEDs

Material System	Energy Gap (eV) at 300 K	Peak Emission Wavelength (Å)
GaAs	1.43 direct	8670 infrared
GaP	2.26 indirect	5485 green
AlAs	2.16 indirect	5740 greenish yellow
InP	1.35 direct	9180 infrared
ZnSe	2.67 direct	4644 blue
GaN	3.42 direct	3626 ultraviolet
SiC (6H)	2.86 indirect	4800 blue
$GaAs_{1-x}P_x$	1.43–2.03 direct	8670–6105 infrared–red
$x_c = 0.49$[a]	2.03–2.26 indirect	6105–5485 red–green
$Al_xGa_{1-x}As$	1.43–1.98 direct	8670–6525 infrared–red
$x_c = 0.43$[a]	1.98–2.14 indirect	6525–5790 red–yellow
$Ga_xIn_{1-x}P$	1.35–2.18 direct	9180–5685 infrared–yellow
$x_c = 0.62$[a]	2.18–2.26 indirect	5685–5485 yellow–green
$(Al_xGa_{1-x})_{0.5}In_{0.5}P$	1.88–2.31 direct	6596–5359 red–green
$x_c = 0.70$[a]	2.31–2.35 indirect	5359–5277 green
GaInAsP	0.724–1.35 direct	17127–9185 infrared
W-InGaN	3.42 and down, direct	4100–5250 violet, blue, green
ZnSeTe	2.67 eV and down, direct	4644–5500, blue and green

[a] x_c is the mole fraction representing the direct–indirect bandgap cross-over point.

LEDs have been produced in large quantities because they are relatively inexpensive and their performance is satisfactory. In an attempt to increase the efficiency of $GaAs_{1-x}P_x$-based LEDs the phosphorus mole fraction in $GaAs_{1-x}P_x$ was increased beyond 0.45 (10). This has the undesirable consequence of causing the band gap to be indirect, which was overcome by introducing isoelectronic nitrogen impurities. When grown on GaP substrate, which is transparent, the light extraction ratio was improved to the point where $GaAs_{1-x}P_x$: N LEDs demonstrated higher luminous performance than both $GaAs_{1-x}P_x$ and GaAs LEDs. However, the performance was still relatively low.

InGaAsP-Based Light Emitting Diodes

The $In_{1-x}Ga_xAs_yP_{1-y}$ quaternary alloy is a potential candidate for light sources for high-luminosity applications. It has a direct energy bandgap of 2.25 eV ($x = 0.74$, $y = 0.0$) at 300 K.

Table 2. Characteristics of Visible LEDs

LED Type	Color (Peak Wavelength, nm)	Typical External Quantum Efficiency (%)	Typical Performance (lm/W)	Bandgap Type	Lattice Matched	Structure[a]	Substrate	Epitaxial Growth Method[b] (p–n Junction Formation)
$GaAs_{0.6}P_{0.4}$	Red (650)	0.2	0.15	Direct	No	Homo.	GaAs	VPE (diffusion)
GaP:(Zn,O)	Red (700)	2	0.4	Indirect	Yes	Homo.	GaP	LPE (grown)
$GaAs_{0.35}P_{0.65}$:N	Red (630)	0.7	1	Indirect	No	Homo.	GaP	VPE (diffusion)
$GaAs_{0.15}P_{0.85}$:N	Yellow (585)	0.2	1	Indirect	No	Homo.	GaP	VPE (diffusion)
GaP:N	Yellow-green (565)	0.4	2.5	Indirect	Yes	Homo.	GaP	LPE (grown)
GaP	Pure green (555)	0.1	0.6	Indirect	Yes	Homo.	GaP	LPE (grown)
$Al_{0.35}Ga_{0.65}As$	Red (650)	4	2	Direct	Yes	SH	GaAs	LPE (grown)
$Al_{0.35}Ga_{0.65}As$	Red (650)	8	4	Direct	Yes	DH	GaAs	LPE (grown)
$Al_{0.35}Ga_{0.65}As$	Red (650)	16	8	Direct	Yes	DH-TS	GaAs	LPE (grown)
$(Al_{0.11}Ga_{0.89})_{0.5}P$	Orange (620)	6[c]	20[c]	Direct	Yes	DH	GaAs	MOVPE (grown)
$(Al_{0.28}Ga_{0.72})_{0.5}In_{0.5}P$	Amber (595)	5[c]	20[c]	Direct	Yes	DH	GaAs	MOVPE (grown)
$(Al_{0.43}Ga_{057})_{0.5}In_{0.5}P$	Yellow-green (570)	1[c]	6[c]	Direct	Yes	DH	GaAs	MOVPE (grown)
SiC (6H)	Blue (480)	0.02	0.04	Indirect	Yes	Homo.	SiC	CVD (grown)
InGaN	Blue (450)	9[d]	3.6	Direct	No	DH	Al_2O_3	MOVPE (grown)
InGaN	Green (525)	6.5[d]	20	Direct	No	DH	Al_2O_3	MOVPE (grown)
ZnTeSe	Green (512)	8[e]	25	Direct	Yes	DH	ZnSe	MBE (grown)

[a] Homo., homojunction; SH, single heterostructure; DH, double heterostructure; DH-TS, double heterostructure with transparent, epitaxially grown substrate (original GaAs substrate removed).
[b] VPE, vapor-phase epitaxy; LPE, liquid-phase epitaxy; MOVPE, metal-organic vapor-phase epitaxy; MBE, molecular beam epitaxy.
[c] Best reported results (30). Typical commercial performance not yet established.
[d] Private communication, Dr. S. Nakamura.
[e] Private communication, Prof. J. Schetzina.

It can be grown on commercial $GaAs_{0.61}P_{0.39}$ epitaxial substrates with exact lattice match in the direct bandgap range of 1.88 to 2.17 eV (660 to 570 nm). Recently, the potential of this alloy system was tested successfully (11) with the fabrication and characterization of $In_{0.32}Ga_{0.68}P/In_{0.12}Ga_{0.88}As_{0.34}P_{0.66}/In_{0.32}Ga_{0.68}P$ double heterostructure LEDs grown on $GaAs_{0.61}P_{0.39}$ substrates by LPE technique. It exhibited a forward-bias turn-on voltage of 1.8 V with an ideality factor of 1.3 and a breakdown voltage of 16 V. The electroluminescent spectra exhibited an emission peak at 620 nm (orange-red) and a FWHM of approximately 15 nm at 20 mA. The external quantum efficiency of 0.22% had been achieved for the bare LEDs.

GaP : N-, GaP : (Zn,O)- and GaP-Based Light Emitting Diodes

GaP : N LEDs emit in the green and exhibit performance somewhat better than $GaAs_{1-x}P_x$: N LEDs. This is because GaP substrate and epitaxial layers are lattice matched and have lower defect density in the bulk. Unlike GaP : N LEDs, GaP : (Zn,O) LEDs emit in the red (9). The zinc and oxygen dopant atoms form a complex of large binding energy, creating a level for carrier transition in the red. In terms of performance, these LEDs are slightly inferior to GaP : N LEDs, although their quantum efficiency is better than that of GaP : N LEDs. GaP can also be employed to form LEDs emitting in the green. These GaP LEDs are dependent, not on nitrogen doping, but rather on phonons to conserve momentum. Furthermore, because the nitrogen recombination centers are absent, the radiative lifetime in these LEDs is higher by an order of magnitude. However, the quantum efficiency was reduced. Nonetheless, the reduction of quantum efficiency was not very large because the absence of nitrogen dopant atoms improves the crystal quality, thus leading to an increase in the nonradiative lifetime τ_{nr}. As the nitrogen traps are not involved in the emission, the emission from GaP LED is also closer to green (555 nm versus 565 nm).

AlGaAs-Based Light Emitting Diodes

The $Al_xGa_{1-x}As$ alloy exhibits a direct energy gap varying between 1.42 eV and 1.70 eV for Al composition $x \leq 0.42$ and hence are used to produce highly efficient red and IR LEDs; the latter type is usually intended for communications applications. LPE is a good technique for the production of $Al_xGa_{1-x}As$ red LEDs. However, a more complex growth technology is necessitated for the growth of the $Al_xGa_{1-x}As/GaAs/Al_xGa_{1-x}As$ double heterostructure LEDs, particularly with thin (1 μm to 3 μm) active regions and ultra thick (>100 μm) confining layers. Almost identical lattice parameters of AlAs and GaAs allow the $Al_xGa_{1-x}As/GaAs$ DH structure to be lattice matched to GaAs substrates. Consequently, heterostructures of various types are grown without any alarming levels of defects, as these efficiency killer defects cannot be tolerated in this material system. Three types of $Al_xGa_{1-x}As$ LEDs are available (12) in large scale: single heterostructure $Al_xGa_{1-x}As/GaAs$ LEDs on GaAs substrate, double heterostructure $Al_xGa_{1-x}As/GaAs/Al_xGa_{1-x}As$ on GaAs substrates, and a double heterostructure $Al_xGa_{1-x}As/GaAs/Al_xGa_{1-x}As$ LEDs with a thick confining $Al_xGa_{1-x}As$ layer but the GaAs substrate removed. Naturally, when the absorbing substrate is removed, the LED performance is enhanced. Unfortunately, the cost also increases with complexity, suggesting that the selection of one type or another LED is very much determined by trade-offs between price and performance.

AlInGaP-Based Light Emitting Diodes

Currently grown by MOVPE technique, $(Al_xGa_{1-x})_yIn_{1-y}P$ and $Al_xGa_yIn_zP$ are important materials for LEDs (13). The simultaneous variations of x and y mole fractions in $(Al_xGa_{1-x})_yIn_{1-y}P$ and of x, y, and z in $Al_xGa_yIn_zP$ allow the emission wavelength to be varied from the visible to IR. Interestingly, the simultaneous variations of x and y mole fractions allow, for example, the $(Al_xGa_{1-x})_yIn_{1-y}P$ alloy system to yield lattice-matched direct bandgap heterostructures for colors other than red. In view of the fact that InP and GaP have lattice parameters approximately equal distances on opposite sides of that of the GaAs substrate, lattice matching requires that the In concentration be kept, as much as possible, close to the sum of the Aluminum and Gallium compositions. Furthermore, Aluminum and Gallium atoms allow the ratio of Aluminum to Gallium to be changed conveniently to form heterostructures. The variations of x and y mole fractions, however, cause $(Al_xGa_{1-x})_yIn_{1-y}P$ to pass through the direct–indirect crossover point in the greener spectral region and at an estimated bandgap energy of 2.31 eV. As shown in Fig. 3, three types of $(Al_xGa_{1-x})_yIn_{1-y}P$ structures are grown to form LEDs. All of these structures are double heterostructures utilizing GaAs substrates. The top window layer is grown relatively thick (about 50 μm) to overcome the limitation imposed by the extraction cone angle by extracting light from the edge of the chip which would otherwise be reflected in. The top window layer could in principle be a higher energy bandgap $(Al_xGa_{1-x})_yIn_{1-y}P$ grown on a lower energy bandgap $(Al_xGa_{1-x})_yIn_{1-y}P$ active layer for transparency and increased cone angle. However, $(Al_xGa_{1-x})_yIn_{1-y}P$ is a relatively high resistivity material and is more costly as well. Thus, for the sake of cost and control over technology, it is replaced by $Al_xGa_{1-x}As$ and GaP. Among $Al_xGa_{1-x}As$ and GaP window layers, $Al_xGa_{1-x}As$ is lattice matched to $(Al_xGa_{1-x})_yIn_{1-y}P$, but absorbs some of the light if it is yellow or green. On the other hand, GaP is transparent and inexpensive, but not lattice matched to $(Al_xGa_{1-x})_yIn_{1-y}P$. Fortunately, the lattice mismatch between GaP and $(Al_xGa_{1-x})_yIn_{1-y}P$ can have limited negative effect because the GaP layer is the last layer grown. It is not surprising that, to date, the best results are obtained in devices utilizing GaP window layers.

In Fig. 4, the external quantum efficiency and luminous performance of $(Al_xGa_{1-x})_yIn_{1-y}P$ LEDs are compared to those of other LEDs (14). The external quantum efficiency of $(Al_xGa_{1-x})_yIn_{1-y}P$ LEDs for wavelengths larger than 590 nm is approximately 5% but falls rapidly for shorter wavelengths as it is affected increasingly by the direct–indirect transition. The luminous efficiency increases with wavelength until approximately 590 nm and then falls off slowly, probably because of changes in the eye sensitivity (see the relative eye sensitivity curve in Fig. 4) and internal efficiency. From Fig. 4, it is apparent that $(Al_xGa_{1-x})_yIn_{1-y}P$ LEDs are superior to other LEDs at least in the wavelength range of 590 nm to 620 nm. They may attain further superiority with technological progress as this technology has been introduced only recently. This is evident from a recent observation that a wafer-bonded visible-spectrum transparent-substrate GaP-AlGaInP/GaP

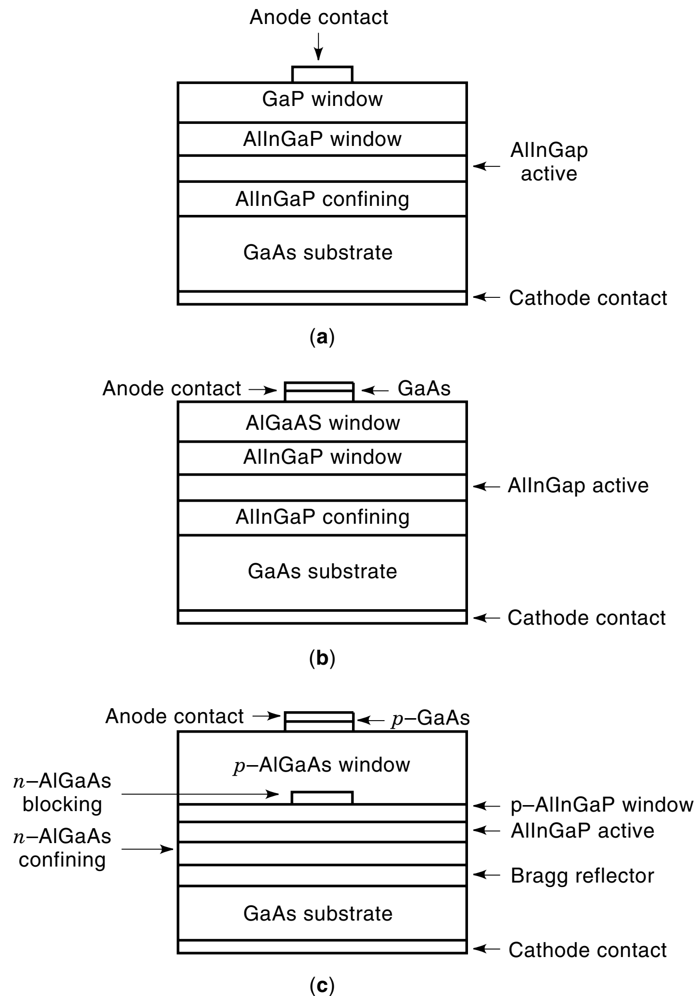

Figure 3. Cross-section of AlInGaP chip structures: (a) GaP window layer, (b) AlGaAs window layer, (c) AlGaAs window layer with a blocking layer beneath the top contact and a Bragg reflector beneath the active layer.

LED is capable of producing a very high external quantum efficiency of approximately 23.7% at 635.6 nm and at an operating voltage less than 2.1 V at 20 mA (15). This is apparent also from the development of $Al_{0.33}Ga_{0.32}In_{0.35}P/Ga_{0.65}In_{0.35}P$ double heterostructure LEDs exhibiting emission wavelengths around 615 nm and an external quantum efficiency of 0.156% at 20 mA (16). There is a good chance that $(Al_xGa_{1-x})_yIn_{1-y}P$ LEDs will demonstrate superb performance for all wavelengths from 550 to 630 nm in the future, and should even surpass AlGaAs at 650 nm if transparent-substrate devices can be developed. Currently, these devices are relatively expensive. However, it is expected that, as the technology is refined, the cost will rapidly decrease.

GaN-Based Light Emitting Diodes

GaN and its alloys with InN and AlN have direct energy gaps that make them suitable for blue LEDs (17). Two problems with GaN growth; namely the nonavailability of suitable substrates and the difficulty of forming *p–n* junctions, have delayed the application of GaN. Currently the most commonly used substrate for GaN growth is sapphire. The advantage of using a sapphire substrate is that it is transparent. The disadvantage of this substrate is that it is very poorly matched both structurally and thermally to GaN, which leads to the generation of high defect density in the bulk. Other substrates such as SiC, MgO, and ZnO used for GaN growth have their own advantages and disadvantages as well. Advancements in low-temperature buffer layers which led to a substantial reduction in defect concentration combined with the nature of a recombination process dominated by localization have all but eliminated the early obstacles as far as standard LED applications are concerned.

One of the early obstacles for achieving *p*-type GaN was the large *n*-type background caused by nitrogen vacancies. Following the reduction of high *n*-type background, *p*-type GaN was produced by MOCVD using Mg as a dopant followed by an electron beam irradiation or a 700°C thermal treatment. Later it was shown that *p*-type GaN can be obtained by molecular beam epitaxy (MBE) without any postgrowth procedure. Following the attainment of *p*-type GaN, GaN based *pn* junction LEDs were developed mainly by two groups in Japan (18,19). Both GaN homojunction LEDs and AlGaN/GaN/AlGaN double-heterojunction (DH) LEDs have been investigated (10% Al in the AlGaN barrier layer). In GaN homojunction LEDs, the dominant emission is in the 430 nm to 480 nm wavelength range (violet to blue) in a relatively broad band (55 nm) originating from the *p*-side. Since the bandgap emission in GaN would be in the UV portion of the spectrum, the said emission inevitably involves the deep levels created by the presence of magnesium, which is used to achieve *p*-type GaN, in the growth environment. The maximum external efficiency reported for the homojunction LED is η_{ex} = 1.5% at 1.5 mW output (30 mA/5 V bias); the maximum output power for DH LEDs was 4 mW for η_{ex} = 0.5% (30 mA bias). Reliability of *p–n* junction LEDs is superior to the older MIS LEDs that have shown a reduction of only 20% in light output after 10^4 h of operation. The early versions of the blue and blue-green LEDs developed by Nichia Chemical Industries,

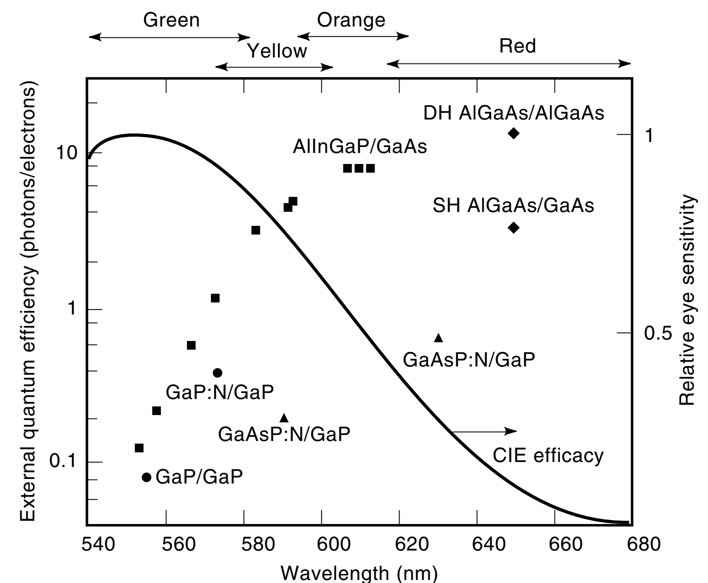

Figure 4. Variation of external quantum efficiency and relative eye sensitivity as functions of peak wavelength of various LEDs. After Craford (14).

Ltd. initially relied on the transitions to deep Zn centers in InGaN (19). This was necessitated by the need to extend the wavelength to the desired values while keeping the InN molar fraction within a level yielding good crystalline quality. These LEDs suffered from wide spectral widths and saturation in the output power with injection current at the intended wavelength of operation. The large spectral width spoiled the color saturation with the undesirable outcome that not all the colors could be obtained through color mixing.

In a more recent development (19), GaInN quantum well (QW) LEDs with GaN barriers have been fabricated by Nichia Chemical Industries, Ltd. With this so called quantum well approach, the InN molar fraction could be increased to about 70%, paving the way for excellent UV, violet, blue, green, and even yellow LEDs. Figure 5 depicts all LED performance throughout the visible range fabricated in conventional III–V, III–nitrides, ZnSe based II–VI semiconductors and organic materials. The performance of organic LEDs is shown as the wide band. The nitride based LEDs exhibit power levels of 5 mW and 3 mW at 20 mA of injection current for the wavelengths of 450 nm and 525 nm, respectively. Very important is the fact that the FWHM of the spectrum was 20 nm and 30 nm for blue and green LEDs, respectively, owing to the fact that these new LEDs take advantage of nearly band-to-band transitions [Fig. 6(a)]. (A detailed investigation of these LEDs shows that the transitions are associated with band tail states.) The In mole fractions used are 20 and 43 for the 450 and 525 nm emission, respectively. The output power as a function of injection current for the blue and green LEDs mentioned above are shown in Fig. 6(b). At the wavelength corresponding to green, 3 mW, which corresponds to 12 cd in a 10° viewing cone, was obtained with an efficiency of 6.3%.

ZnSe-Based Light Emitting Diodes

Semiconductor materials such as alloys ZnS and ZnSe from columns II and VI of the periodic table have direct energy band gaps exceeding 2.5 eV. These are, therefore, suitable for blue LEDs (20). Over the years, several shallow acceptors were considered to be suitable for ZnSe. This process was assisted by a gradual reduction of unwanted background impurities to a level of less than $10^{14}/cm^3$. The availability of purified zinc and selenium sources and the advancement in the MBE growth of ZnSe led to a better control of the background donor concentration, and also provided consistency in quality layers. One major advantage of ZnSe materials is that, unlike GaN, they can be nearly lattice matched to GaAs substrates. As in the case of wide gap nitrides, ZnSe based material systems also suffered from the lack of *p*-type material. With the attainment of *p*-type ZnSe through the use of activated nitrogen sources, fabrication of LEDs emitting in the blue-green spectral region became possible. However, these devices suffer from reliability problems. The main disadvantage is the poor covalent bond strength that leads to defects in the presence of high-energy photons.

To overcome the difficulty of *pn* junction LEDs, short-period superlattice (SPSL) LED structures grown by MBE have also been tried for blue emission. The devices consisted of an ZnSe active layer, SPSL MgZnSSe cladding layers and a ZnSe/ZnTe digitally graded contact layer. High purity blue emission occurred at 460 nm at room temperature with a 13 nm full width at half maximum. Operating at 14 A/cm^2, the half-intensity lifetime of the LED was more than 13 h at room temperature and the external quantum efficiency was about 0.1%.

The above ZnSe-based LEDs were realized on GaAs substrates with reliability falling short of requirements. In addition, the substrate absorbs the radiation reducing the light intensity that can be extracted. The short lifetimes have been attributed to stacking faults, which presumably were overcome by utilizing ZnSe substrates. Additionally, the luminous efficiency of approximately 25 lm/W at green was also obtained. This breakthrough came about through a collaborative effort between Prof. Schetzina of North Carolina State University and Eagle Picher of Miami, Oklahoma. The ZnSe/ZnTeSe/ZeSe double-heterostructure LEDs emitting at 512 nm exhibited a spectral half-width of 40 nm, and an output

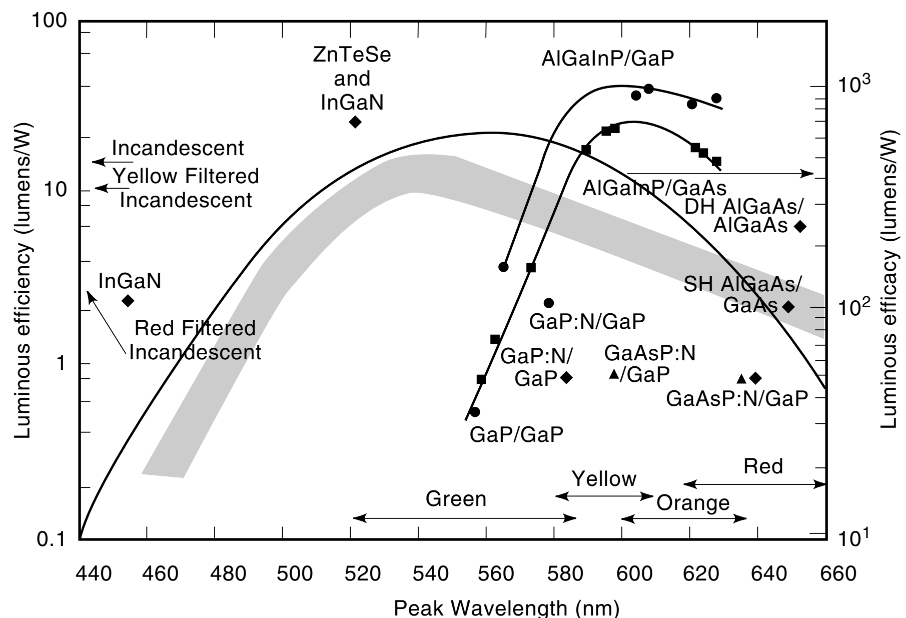

Figure 5. Light emitting diode performance throughout the visible range fabricated in conventional III–V, III–nitrides, ZnSe based II–VI semiconductors, and organic materials. The performance of organic LEDs is shown as the wide band. Also shown is the eye efficacy.

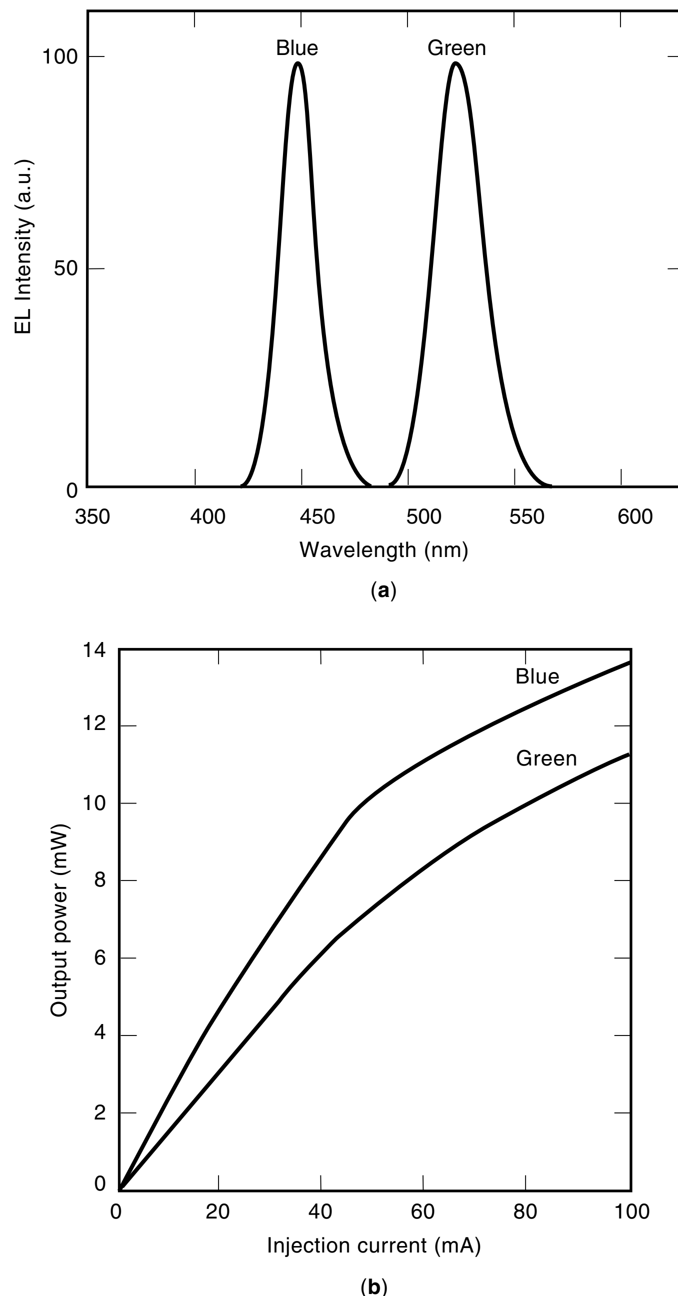

Figure 6. (a) Electroluminescence of blue and green single quantum well InGaN/GaN LEDs at a forward current of 20 mA. (b) The output power of blue and green single quantum well InGaN/GaN LEDs as a function of forward current. Courtesy of Dr. S. Nakamura, Nichia Chemical Industries, Ltd.

power of 1.69 mW at 10 mA. The diode voltage was 2.4 V, the external quantum efficiency and power efficiency (wall plug efficiency) of 6.9% and 6.5%, respectively, and an operation lifetime of greater than 10,000 h have been attained. Due to low resistance, ohmic contact, and reduced carrier leakage, the quantum efficiency and wall plug efficiency were very similar.

SiC-Based Light Emitting Diodes

6H-SiC is a column IV material with an indirect energy bandgap of 2.86 eV. The common procedure for forming these devices is to grow epitaxial SiC on SiC substrates by using sublimation VPE or LPE technique. Because SiC can be easily doped *p*-type by using aluminum dopant atoms, and *n*-type by using nitrogen dopant atoms, *pn* homojunctions can be readily obtained. The major problem with this material is that it has an indirect energy bandgap which causes the efficiency to be relatively low. Yet, the light output has steadily improved as the material growth technology underwent a series of refinements. To overcome the difficulties resulting from its indirect energy bandgap, various isoelectronic impurities have been added over the years. The effort has been reasonably successful in the sense that SiC thus has been made to show electroluminescence across the entire visible spectrum. The SiC blue LEDs developed recently by Cree Research Inc. (22) exhibit blue emission centered at 470 nm Fig. 7(a) and (b)]. These devices radiate optical power levels of approximately 18.3 μW at 25 mA (3 V) with a spectral half-width of 69 nm and an efficiency in the range of 0.2% to 0.03% with recently released devices exhibiting even higher power and better efficiencies. Fortuitously, low efficiency and power is somewhat compensated for by operating these robust SiC LEDs at high currents. For example, 36 μW of output power has been achieved at a current level of 50 mA. At this current level, typical degradation of these LEDs is only 10% to 15% over 10^4 h, which is significantly less than what is observed with GaP LEDs. Other groups at Siemens AG, Sanyo, and Sharp have also been successful in developing prototype devices. However, to our knowledge, they have not yet reached the status achieved by Cree's blue LEDs. The primary light-producing mechanisms have been identified to be donor-to-acceptor (DA) recombination (480 nm), bound exciton recombination at localized aluminum centers (455 nm) and free exciton recombination (425 nm). Importantly, it is found that the key to reaching shorter wavelengths is to reduce the background nitrogen contamination. The reduction in background nitrogen contamination leads to an increased exciton-related luminescence. If measures are taken to increase the power levels significantly, the efficiency decreases probably because of a saturation of the DA levels. To curtail this problem, it may, therefore, be necessary to increase DA density, which would result in an overall increase in the high-power efficiency of SiC LEDs. The advent of GaN-based LEDs operating in blue and green are certain to make SiC obsolete.

Organic Light Emitting Diodes

Organic semiconductors are nowadays increasingly used to make visible LEDs. Unlike LEDs from inorganic semiconductors, those from organic semiconductors can be designed as large-area light-emitting panels that are operative at low drive voltages. Generation of light in these materials takes place from the recombination of holes and electrons injected from the electrodes. Such recombination in the emitting layer then excites the emitter material. The emitter layer can either be low-molecular-weight materials or high-molecular-weight polymers. Among polymers, conjugated semiconducting polymers in particular have been widely used as the emitting layer in LEDs. One perfect example is poly(1,4-phenylenevinylene), which yields green color emission and other colors of longer wavelengths (23). Nonconjugated polymers such as poly(methyl methacrylate), which are abbreviated as PMMA, are also used as the emitter layers in LEDs

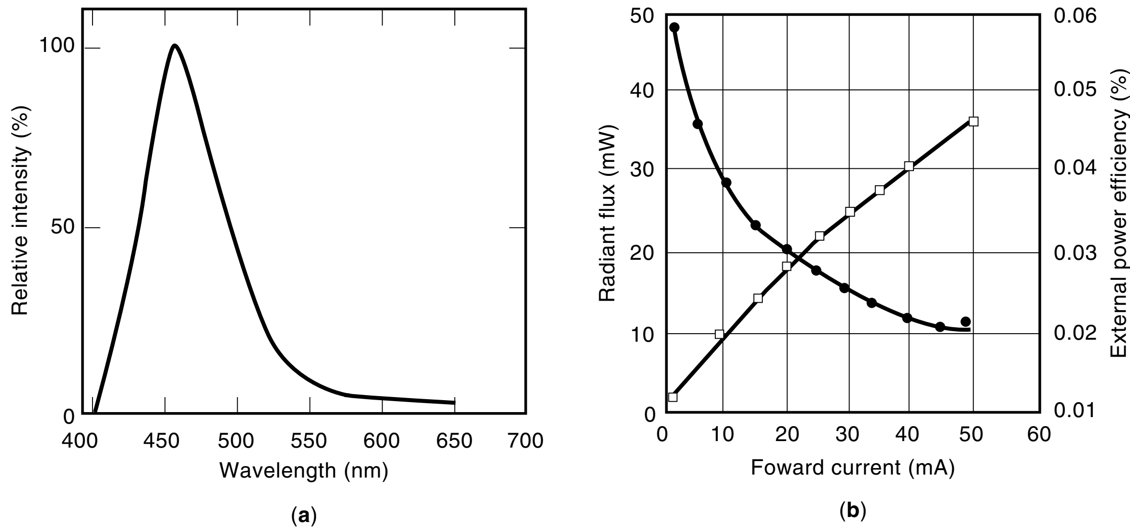

Figure 7. (a) Variation of relative intensity as a function of wavelength of Cree Research SiC LEDs. (b). Variation of radiant flux (small squares) and efficiency (small solid circles) with forward current in Cree Research SiC LEDs.

(24). Blue emission peaking at 410 nm and a luminance of 700 cd/m^2 were achieved from poly(*N*-vinylcarbazole) LEDs (25) at a drive voltage of 14 V. Figure 8 shows a schematic representation of one such organic LED with the light being collected through the transparent glass substrate.

INFRARED LIGHT EMITTING DIODES

Infrared LEDs are most commonly used for communication applications and sport various configurations, some similar to the visible LEDs some designed specifically for coupling to optical fibers. For communication applications, the interest is in the 0.85, 1.3, and 1.5 μm regions, which can be attained with the AlGaAs ternary and InGaAsP quaternary alloys. The advantages of LEDs over lasers for optical fiber communications are their smaller temperature dependence, higher temperature operation, simpler device designs and simpler drive circuits. The disadvantages include lower modulation bandwidth and light intensity and wider spectral line widths (26).

The IR LEDs also utilize basically two kinds of configurations, namely, the surface and edge emitting types. Of course, in the instant case, the goal is to couple the light to a small optical fiber. The surface emitters rely on a well etched into the substrate side of the diode material in such a way as to allow insertion of the fiber (27). The edge emitters are very similar to lasers with built in optical guides. The optical fiber must be butted against the edge of the diode where the light exits the semiconductor. The direct beam nature of the emission in edge emitters increases the coupling efficiency to a fiber with small acceptance angle.

The frequency response of an IR LED is an important factor and must be taken into consideration in the device design. The ultimate modulation bandwidth is determined by the carrier lifetime. The frequency response of LEDs can be described by a single pole circuit as

$$|P(\omega)|^2 = \frac{[P(0)]^2}{1 + (\omega\tau_r)^2} \tag{10}$$

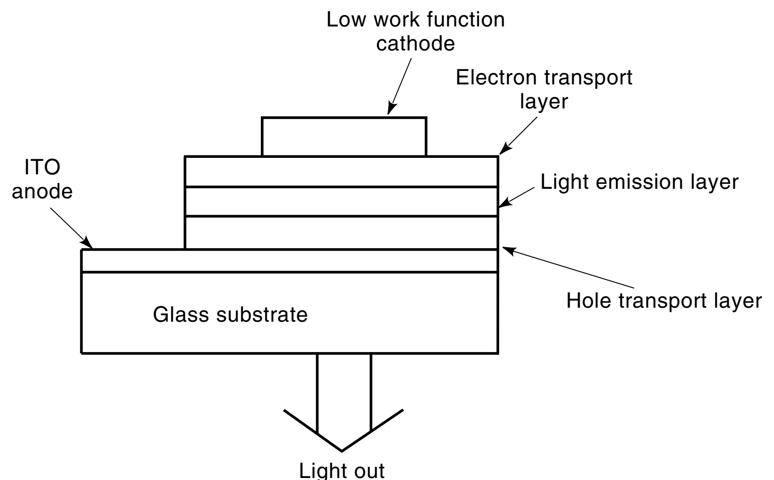

Figure 8. Schematic diagram of an organic LED on a glass substrate.

where $P(\omega)$ and $P(0)$ represent the optical power emitted at frequencies of ω and dc, and τ_r is the overall carrier lifetime. The 3 dB point or the frequency at which the optical power drops to half of its low-frequency value is defined as the modulation bandwidth or the cut-off frequency and is given by

$$f_c = \frac{1}{2\pi\tau_r} \tag{11}$$

The injected carrier concentration is related to injected current through

$$\Delta n = \frac{J\tau_r}{qw} \tag{12}$$

where w and J represent the active layer thickness and the current density, respectively. Utilizing $\tau_r^{-1} = B\Delta n$, we obtain for the cut-off frequency

$$f_c = \frac{1}{2\pi}\left[\frac{BJ}{qw}\right]^{1/2} \tag{13}$$

Clearly, the cut-off frequency is proportional to the square root of the recombination rate and current density product. It is inversely proportional to the square root of the active layer thickness. Note that the above expressions have been derived under the assumption that the recombination is a bimolecular process and that the doping level in the active layer is light. Modulation bandwidths of about 1 GHz (28) and 1.2 GHz (29) are possible with increased doping as it increases the recombination rate and reduces the carrier lifetime in AlGaAs and InGaAsP LEDs, respectively. Reducing the carrier lifetime with creation of nonradiative recombination centers also reduce the light intensity for a given current and should be used as a last resort.

CONCLUSIONS

The prospects and progress of visible LEDs have been reviewed. It appears that, among various LEDs, the (In,Ga)N LEDs, which show high performance in the green to violet region of the optical spectrum have great potential for further improvement. Organic/polymeric LEDs will also expand their bases, particularly indoor active display and background lighting applications, chiefly because of their cost effectiveness and large area capabilities. Recent development of GaN-based blue-green LEDs permits the fabrication of full-color, large-area, sunlight-viewable flat-panel displays, traffic lights, and moving signs. With further improvements in blue and red primary colors, it may be possible for LED to make inroads in lighting applications.

ACKNOWLEDGMENTS

One of us, H.M. has been supported by funds from ONR and AFOSR with grants monitored by Drs. G. L. Witt, C. E. C. Wood, Y. S. Park, and Mr. M. Yoder. H.M. would also like to thank Drs. A. Garscadden, P. Hemenger, and C. Litton for their hospitality during his stay at Wright Laboratories, and Dr. S. Lester for fruitful discussions and facts and figures that were used in constructing some of the figures contained in this chapter.

BIBLIOGRAPHY

1. H. Morkoç and S. N. Mohammad, *Science* **267**: 51–55, 1995.
2. R. H. Saul, J. Armstrong, and W. H. Hackett, *Appl. Phys. Lett.* **15**: 229, 1969.
3. R. A. Logan, H. G. White, and W. Wiegmann, *Appl. Phys. Lett.* **13**: 139, 1968.
4. W. O. Groves, A. H. Herzog, and M. H. Craford, *Appl. Phys. Lett.* **19**: 184, 1971. M. G. Crawford, R. W. Shaw, R. W. Groves, and W. O. Herzog, *J. Appl. Phys. Phys.* **43**: 4075, 1972.
5. Z. I. Alferov et al., *Sov. Phys. Semicond.* **6**: 1930, 1973.
6. R. D. Dupuis and P. D. Dapkus, *Appl. Phys. Lett.* **31**: 466, 1977.
7. J. A. Edmond, H. S. Kong, and C. H. Carter, Jr., *Physica B,* **185**: 453, 1993.
8. M. Hegerott et al., *Appl. Phys. Lett.* **62**: 2108, 1993.
9. R. H. Saul, T. P. Lee, and C. A. Burrus, in W. T. Tsang *Semiconductors and Semimetals,* Vol. 22, Part C, Orlando, FL: Academic Press, 1985, pp. 193–237.
10. A. H. Herzog, D. L. Keune, and M. G. Craford, *J. Appl. Phys.* **43**: 600, 1972; A. H. Herzog, W. O. Groves, and M. G. Craford, *Appl. Phys. Lett.* **40**: 1830, 1969.
11. C.-W. Chen and M.-C. Wu, *J. Appl. Phys.* **77**: 905, 1995.
12. J. Nishizawa and K. Suto, *J. Appl. Phys.* **48**: 3484, 1977. L. W. Cook, M. D. Camras, S. L. Rudaz, and F. M. Steranka, *Proc. 14th Int. Symp. GaAs Related Compounds,* 777–780, Bristol: Institute of Physics, 1988.
13. D. S. Cao and G. B. Stringfellow, *J. Electron. Mater.* **20**: 97, 1990; F. A. Kish et al., *Appl. Phys.* **64**: 2839, 1994.
14. M. G. Craford, *IEEE Circuits and Devices,* **8**: 24, 1992.
15. G. E. Hofler et al., *Appl. Phys. Lett.* **69**: 803, 1996.
16. J.-F. Lin et al., *J. Cryst. Growth* **137**: 400, 1994.
17. S. N. Mohammad and H. Morkoç, *J. Prog. Quantum. Electron.* **20**: 361, 1996.
18. H. Amano, T. Ashai, and I. Akasaki, *Jpn. J. Appl. Phys.* **29**: L205, 1990.
19. S. Nakamura, M. Senoh, and T. Mukai, *Jpn. J. Appl. Phys.* **30**: L1701, 1991; S. Nakamura, T. Mukai, and M. Senoh, *Appl. Phys. Lett.* **64**: 1687, 1994; S. Nakamura, T. Mukai, and M. Senoh, *J. Appl. Phys.* **76**: 8189, 1994; S. Nakamura, M. Senoh, N. Iwasa, S. Nagahama, T. Yamada, and T. Mukai, *Jpn. J. Appl. Phys.* **34**: L1332, 1995.
20. M. A. Haase et al., *Appl. Phys. Lett.* **58**: 1272 (1991); J. Jeon et al., *Appl. Phys. Lett.* **60**: 892, 1992.
21. B. J. Wu et al., *Appl. Phys. Lett.* **68**: 379, 1996.
22. J. A. Edmond, H. S. Kong, and C. H. Carter, Jr., in C. Y. Yang, M. M. Rahman, and G. L. Harris, eds. *Amorphous and Crystalline Silicon Carbide IV,* Berlin: 344–351, Springer, 1992.
23. J. H. Burroughes et al., *Nature* **347**: 539, 1990; P. L. Burn et al., *Nature* **356**: 47, 1992; A. R. Brown et al., *Appl. Phys. Lett.* **61**: 2793, 1992; P. L. Burn et al., *J. Chem. Soc., Chem. Commun.* 32, 1992; A. R. Brown et al., *Chem. Phys. Lett.* **200**: 46, 1992.
24. J. Kido et al., *Appl. Phys. Lett.* **61**: 761, 1992.
25. J. Kido et al., *Appl. Phys. Lett.* **63**: 2627, 1993.
26. S. Soul, *IEEE Trans. Electron Devices,* **ED-30**: 285, 1985.
27. C. A. Burns and B. I. Miller, *Opt. Comm.* **4**: 307, 1971.

28. J. Heinen, W. Huber, and W. Harth, *Electron. Lett.* **12**: 553, 1976.
29. H. Grothe, W. Proebster, and W. Harth, *Electron. Lett.* **15**: 702, 1979.
30. Huang et al., 1992.

S. Noor Mohammad
Howard University
Hadis Morkoç
Virginia Commonwealth University